

AERODYNAMIC STABILITY OF TWO CABLE-STAYED BRIDGES

Harold R. Bosch and Lloyd R. Cayes, Federal Highway Administration

The trend in long-span bridge development has been toward increased spans and flexibility and decreased dead weight and damping through use of higher strength materials, refinements in design procedures, and modern fabrication techniques. In some cases, this makes the structure, especially cable-stayed and suspension bridges, sensitive to wind-induced oscillations. Three types of vibrations, namely flexural, torsional (or coupling of the two), and flutter, should be investigated in the design. There is presently no purely analytical or theoretical procedure for the investigation of any of these types of oscillations. Aerodynamic stability information must be obtained from field observations or wind tunnel testing of models. Cable-stayed bridge concepts are receiving popularity in this country. Current cable-stayed designs are subject to the same fundamental wind excitation as the classical suspension bridge; however, the inherent increase in stiffness of the cable-stay box-girder does place it in a different realm of response. With this in mind, several wind tunnel aerodynamic studies have been conducted and recently completed. This paper discusses the results of two such studies. Information is presented regarding vortex shedding response amplitude and acceleration, critical flutter velocity, flutter derivatives, and static force coefficients.

This paper describes the procedures and presents the results of wind tunnel aerodynamic investigations of two cable-stayed bridges presently under construction in the United States. The first bridge investigated is a four-lane structure comprised of double trapezoidal steel box girders with an orthotropic deck and will cross the Mississippi River at Luling, Louisiana. The second is a two-lane structure with a single steel box and will cross the Ohio River at Huntington, West Virginia. Elevation and cross-sectional views are presented in Figures 1 and 2. Both studies were conducted in the George S. Vincent Wind Tunnel by the Federal Highway Administration (FHWA) for the Louisiana Department of Transportation and Development and West Virginia Department of Highways, respectively.

The objective of each investigation was to determine bridge dynamic deflection and acceleration under vortex shedding excitation and the critical wind velocity for flutter instability.

It has been well known for many years that serious vibration problems can arise with suspended bridge structures as a result of wind action. Perhaps one of the earliest well documented examples is the failure of the Brighton Chain Pier Bridge in England in 1836 which was witnessed and reported on by Lt. Col. William Reid of the British Army. In fact, as noted by Farquharson (1), 10 suspension bridges suffered major damage or total collapse during the period 1818 to 1889. Most of these failures were of bridges of relatively short spans.

The half century following the 1889 failure of the 384.1-m (1,260-ft) span Niagara-Clifton Bridge marked a period of rapid advances in design and construction techniques as well as materials production and led to the appearance of lighter structures with significantly increased span lengths. The original Tacoma Narrows Bridge was the product of such progress, and its dramatic failure in 1940 is, perhaps, the best known example of an aeroelastic bridge deck instability. Investigations into the causes of the Tacoma Narrows disaster were immediately undertaken at the University of Washington (1), where wind tunnel tests on a scale model reproduced quite faithfully the observed behavior of the bridge during its brief life. The stability of the proposed design for the new bridge was then established by wind tunnel testing. Further research revealed that a section model representing a limited length of the bridge and mounted on springs to reproduce to scale the frequency of a significant mode of motion could be used to determine the response of the bridge in a normal wind at various vertical angles of attack.

During the past decade there has been considerable interest in employing wind tunnel techniques for the determination of the aerodynamic stability derivatives of suspended bridge models (2). These derivatives represent purely aerodynamic data, as opposed to overall dynamic response observations, which are the consequence, uniquely, of bridge cross section geometry.

In earlier wind tunnel tests, bridge deck section models were elastically suspended, with properly scaled vertical and torsional natural frequencies, and observed primarily for their

tendencies to flutter at some air speed. The present practice is to extract the purely aerodynamic characteristics of the model first and then employ these in the dynamic response calculations for the full bridge. This practice has the inherent advantage of divorcing test results from all model structural properties, such as inertia, damping, and frequency, except for geometry.

There are two basic types of wind effects on structures, static and dynamic. The static effect is the pressure that the moving air mass exerts against the structure, and it varies in direct proportion to the square of the mean velocity. The dynamic effects are the forces generated by flow separation and turbulence of the moving air as it passes around the structure or by changes in wind speed such as gusting.

In consideration of the static stability of bridge structures under steady wind, the critical wind direction is normally taken to be perpendicular to the longitudinal axis of the bridge. Lift, drag, and moment coefficients are estimated or measured in the wind tunnel for use in calculating the respective uplift, side thrust, or twist forces on the structure. When lift or drag forces become excessive, an unstable bridge may undergo lateral buckling or torsional divergence.

One form of wind-induced vibrations of bridges is that of vortex shedding response. When wind blows across a slender, bluff object, such as a bridge superstructure, the large wake that is formed consists of an array of vortices which are spaced in a characteristic pattern. The vortices form alternately on either side of the body in a periodic fashion, with the shedding frequency proportional to wind speed. The fluctuating nature of the wake causes an oscillatory force on the bridge, and as shedding frequency approaches the natural frequency of the structure, it is possible for vibrations to result. This response occurs over a range of wind velocities in the vicinity of the resonant value, with maximum amplitude obtained when the "lock-in" condition is achieved. Both the velocity range and maximum amplitude are functions of structural damping and degree of streamlining. Since vortex shedding response is amplitude limited, structural problems arising from this mechanism are seldom catastrophic, although local fatigue damage and human discomfort are possible and warrant consideration.

Another form of instability, and perhaps the most important, is commonly referred to as flutter, following terminology developed in early work on aeroelastic instabilities of aircraft. In this case, wind forces interact with bridge deck motions to create a self-excited oscillation of growing amplitude, possibly leading to destruction. Unlike the vortex shedding problem, the flutter phenomenon is not limited to a velocity range beyond which structural stability returns. Increasing velocity beyond the threshold value causes oscillations to buildup more rapidly and leads to more violent action.

Basic Theory and Mathematical Modeling

The susceptibility of the prototype structure to aerodynamic instability is determined by wind tunnel tests. These tests are conducted on a section model of the bridge which is subjected to laminar flow.

To extract detailed aerodynamic derivative data from the wind tunnel section model studies, it is necessary to provide an analytical model of the physical situation. For this purpose, a symmetrical

two-degree-of-freedom system is assumed. As discussed by Scanlan (3), the equations of motion for the sectional structure may be written in the form:

$$m \left(\ddot{h} + 2\zeta_h \omega_h \dot{h} + \omega_h^2 h \right) = L \quad (1)$$

$$I \left(\ddot{\alpha} + 2\zeta_\alpha \omega_\alpha \dot{\alpha} + \omega_\alpha^2 \alpha \right) = M \quad (2)$$

where I and m are mass moment of inertia and mass per unit span of model; h and α are vertical and torsional deflections of the given deck section (assumed uniform); ζ is the damping ratio-to-critical; ω is the circular frequency; and L and M are the dynamic lift and moment per unit span. For the self-excited flutter problem, L and M are taken as linear functions and may be written in the form:

$$L = m \left(H_1 \dot{h} + H_2 \dot{\alpha} + H_3 \alpha \right) \quad (3)$$

$$M = I \left(A_1 \dot{h} + A_2 \dot{\alpha} + A_3 \alpha \right) \quad (4)$$

where H_i and A_i ($i = 1, 2, 3$) are dimensional aerodynamic derivatives determined by experiment, with inertial factors introduced for convenience. By noting the fact that L and M are essentially functions of the "reduced frequency" or dimensionless parameter $K = B\omega/U$, nondimensional derivatives or coefficients may be obtained as:

$$L = 1/2 \rho U^2 (2B) \left(KH_1^* \frac{\dot{h}}{U} + KH_2^* \frac{B\dot{\alpha}}{U} + K^2 H_3^* \alpha \right) \quad (5)$$

$$M = 1/2 \rho U^2 (2B) \left(KA_1^* \frac{\dot{h}}{U} + KA_2^* \frac{B\dot{\alpha}}{U} + K^2 A_3^* \alpha \right) \quad (6)$$

where H_i^* and A_i^* ($i = 1, 2, 3$) are nondimensional aerodynamic coefficients; B is deck width; U is oncoming wind velocity; and ρ is air density. These equations have been reduced to experimental form to enable direct use, and the details of this reduction are included in reference 3. Essentially, test observations produce time histories of h and α ; then with all quantities on the left-hand sides of equations 1 and 2 known, the coefficients are matched by system identification techniques to the test observations as functions of K .

The coefficients are important in evaluating the stability characteristics of a section. The A_2^* coefficient measures aerodynamic damping in the torsion mode and thus is an indicator of single-degree flutter in that mode. The A_3^* coefficient is usually small and is sometimes assumed zero in analysis. In general, it is a measure of the aerodynamic stiffening effect upon frequency. The H_1^* coefficient measures the aerodynamic damping in the vertical mode.

When vortex shedding response is exhibited either indirectly in the aerodynamic coefficients or directly in observations of the model test, the aforementioned mathematical model must be augmented to be applicable to the region of response (4). This can be done for the case of purely vertical motion by providing equation 5 with a special forcing function:

$$L(t) = \frac{1}{2} \rho U^2 (2B) C_{L0} \sin \omega_s t. \quad (7)$$

The resulting combined equation takes on the form:

$$m \left(\ddot{h} + 2\zeta_n \omega_n \dot{h} + \omega_n^2 h \right) = \frac{1}{2} \rho U^2 (2B) \quad (8)$$

$$x \left(K \frac{h^*}{U} + C_{L0} \sin \omega_s t \right)$$

where H_0^* is an aerodynamic damping coefficient for decay to a resonant response amplitude; C_{L0} is an oscillating lift coefficient; and ω_s is the Strouhal circular frequency. It should be noted here that a completely analogous model could be developed for the torsional case. The parameters above are determined experimentally from records of oscillations at the vortex "lock-in" condition and enable the ultimate prediction of prototype response amplitude.

The "strip" equation for the prototype deck section is expressed as:

$$M \left(\ddot{\eta} + 2\gamma_s \omega_s \dot{\eta} + \omega_s^2 \eta \right) = P \sin \omega_s t, \quad (9)$$

and the maximum mid-span amplitude is computed as:

$$\eta_{\max} = \frac{P}{2M \omega_s^2 \gamma_s} \quad (10)$$

$$\text{where } \gamma_s = \zeta - \frac{\rho B^2 H_0^*}{2m}$$

$$P = \rho U^2 B C_{L0} \int_{\text{span}} \psi(x) dx = \text{generalized force amplitude,}$$

$$M = m \int_{\text{span}} \psi^2(x) dx = \text{generalized mass,}$$

$\psi(x)$ = normalized span deflection.

$\psi(x)$ is approximated by assuming that the main span deflected shape is represented by a half wave sine curve.

Design and Construction of Models

A section model of a suspended bridge superstructure is a geometrically similar copy of a typical length of the suspended structure only. Any cables or hangers are not modeled because their aerodynamic effects are considered negligible. The section model is rigidly constructed to ensure that all elastic behavior takes place in the springs from which it is suspended. The vertical and rotational movement of the section model supported by its spring suspension simulate the vertical bending and torsional twist of the prototype structure.

Four basic section models with 15 potential configurations were designed and constructed for the Luling test program. All models were designed to a geometric length scale of 1:60 to ensure adequate reproduction of significant structural details. Model length was set at 1.524 m (60 in) inside to inside of end plates, representing a 91.46-m (300-ft) section of prototype span. Model widths vary from .4281 m (16.85 in) to .5070 m (19.95 in), resulting in aspect ratios between 3.56 and 3.00. Details are given in Table 1 and illustrated in Figure 3.

For the Huntington test program, one basic section model with five potential configurations was designed and constructed to a scale of 1:45, with the 1.524-m (60-in) length representing 68.58 m (225 ft) of prototype. The width of the model is

.2446 m (9.6 in), resulting in an aspect ratio of 6.25. Details are given in Table 1 and illustrated in Figure 3.

End plates were employed so that two-dimensional flow could be maintained near the model ends. The models were scaled according to Froude number criterion for wind speed and vertical natural frequency. Due to practical limitations of simulating the relatively high prototype torsional characteristics, torsional natural frequency does not, however, achieve Froude scaling.

To maintain proper weight and weight distribution, develop sharp edges, and provide necessary model strength and rigidity, a variety of lightweight materials were incorporated into the model designs. Girder webs, floor beams, and asphalt decks are constructed of aircraft birch plywood. Girder and beam flanges, edge strips, and railing lips are aluminum. Balsa wood was used for diaphragms, ribs, traffic barriers, stiffeners, and concrete decks. The end plates are of "sandwich" construction, with balsa wood between aluminum sheets. Edges were tapered to reduce drag effects, and an elliptical shape was chosen to minimize weight and polar mass moment of inertia. Trusses with tubular aluminum members were extended from the end plates to provide crossbars 2.286 m (90 in) apart for attachment of the supporting springs. Traffic barriers are attached with machine screws to facilitate removal for modification of the cross section. Details of the experimental arrangement can be seen in Figure 4.

Test Procedure and Instrumentation

The tests were conducted in the FHWA open circuit, low velocity wind tunnel which was designed particularly for testing bridge section models. A blower forces air through a diffusing section with a series of stainless steel wire screens into a cylindrical pressure chamber and through the nozzle from which the air is discharged onto the model. The velocity over the cross section of the wind stream is very uniform to a point 1.8 m (6 ft) beyond the end of the nozzle.

A steady wind velocity, with a range of 0 to 9.1 m/sec (0 to 30 ft/sec), is maintained with a micro-control rheostat in the blower circuit. The wind velocity is computed from the dynamic pressure head of the wind stream obtained by direct measurement with a pitot-static tube and an inclined manometer. Corrections are made for changes in air or fluid temperature and barometric pressure.

The nozzle can be rotated about the horizontal axis of the pressure chamber, allowing tests at various wind angles of attack. The angle of attack is the vertical angle between the wind velocity vector and a horizontal plane; a positive angle of attack indicates an upward wind.

The section models were suspended in front of the wind tunnel nozzle by means of four supports with upper and lower coil springs at each support, as illustrated in Figure 4. The vertical length of the springs was adjusted to set the proper vertical frequency of oscillation. The torsional frequency was set by adjusting the spacing between the springs at each end of the model. Although it was not possible to attain the relatively high torsional frequency desired, attempts were made to obtain as high a frequency as possible. The total mass of the section model, end plates, support trusses, end bracket crossbars, and "moving" springs was tuned to the desired scaled quantity by the addition of small weights to the end plates at the model center of gravity.

Horizontal restraining wires were attached to the end bracket crossbars at the center of gravity of the model to prohibit longitudinal or lateral movement during the tests. The restraining wires, which were tensioned with 0.9-kg (2-lb) weights, were of sufficient length that their vertical components would have no significant effect upon the vertical or torsional motion of the model.

Electrical resistance strain gages were attached to beryllium copper flexure plates above the coil springs. The strain gages at one end of the model were wired to indicate the vertical component of oscillation, and those at the other end were wired to indicate the torsional component. Strain gage outputs were amplified and the two components were recorded side-by-side on an oscillograph.

The models were tested only under laminar flow conditions. The tests were conducted at wind angles of attack varying from $+6^\circ$ to -4° . While maintaining a steady wind velocity at each of a series of increasing values, the models were displaced in the respective vertical and torsional degrees-of-freedom, released, and the oscillatory dynamic response recorded. For the vertical mode, the initial displacement was accomplished manually. For torsion, however, it was necessary to "hold" the model at a 4° displacement and release it using solenoids. The velocity and response data were processed on the FHWA computer system to obtain the aerodynamic derivatives and vortex response information discussed earlier.

The damping values of the model setup were determined by displacing and then releasing the model in a no-wind condition and recording the rate of decay. For the Luling study, tests were conducted at the values of model damping exhibited, and results were extrapolated for other values of damping as necessary. In the Huntington tests, however, various amounts of artificial damping were added during testing to yield results for a range of damping values.

Discussion of Results

Test results for each of the seven Luling configurations and the one Huntington configuration (Model 3-2.4-.01) are summarized in Figures 5 through 10.

No vertical flutter (self-excited, divergent, vertical oscillations) was exhibited by any of the model configurations during laboratory testing. This observation is verified by the computer plots of the aerodynamic derivatives. The H_1 derivative, the function for aerodynamic damping of vertical oscillations, shows positive damping over the full test range. A typical plot of this derivative is presented in Figure 5. Torsional critical flutter velocities at zero damping and 1 percent damping are illustrated for prototype wind speed and wind angle (angle of attack) in Figures 6 and 7. Torsional flutter (self-excited, divergent, torsional oscillations) was exhibited at horizontal wind speeds greater than equivalent prototype design requirements of 240 km/h (150 mph) for Luling and 200 km/h (125 mph) for Huntington. The greatest flutter stability was demonstrated by the most "streamlined" models, C-6-C-A, C-6-C-B, and C-2C-A, with critical velocities in excess of 400 km/h (250 mph). As angle of attack increases in the positive direction, flutter stability generally decreases for the Luling configurations. Flutter stability of the Huntington model, however, is insensitive to angle of attack.

Since high wind velocities at high angles of attack are not considered likely in view of data

obtained at the Severn and Newport Bridges (5), critical flutter velocities of less than design wind speed at high angles of attack are not considered a point of concern. Again, these observations are verified by computer plots of the A_2 derivative, indicative of torsional aerodynamic damping. When A_2 becomes positive, self-excitation tendencies are restrained only by the structural damping. A typical plot of this derivative is presented in Figure 8.

An excitation of the bridge deck in vertical and torsional modes by the resonant action of the periodic shedding of vortices in the wake of the structure was exhibited by all models. This amplitude-limited oscillation can be an unacceptable characteristic of the design when it occurs at moderate wind speeds, and resulting accelerations could be disturbing to the user. Generally, vertical vortex shedding response was exhibited at various velocities or ranges of velocities between 24 and 48 km/h (15 and 30 mph), while torsional vortex shedding response was exhibited between 96 and 160 km/h (60 and 100 mph). Since torsional response occurs at relatively high velocities, its effect on the user may be disregarded. For the vertical response which occurs at moderate wind speeds, deck accelerations of 2 percent of "G" are considered acceptable. Estimates of prototype accelerations are illustrated in Figure 9 for vertical response in a horizontal wind. Models C-2C-C and C-2C-A demonstrated the least overall vertical response, while the Huntington model, 3-2.4-.01, exhibited the most. These estimates are considered conservative since it is probable the real wind over the bridge span will be gusty enough to cause poor spanwise correlation and decrease the likelihood of "lock-in" to occur.

Drag coefficients were obtained for the preferred Luling cross section, C-2C-A, and its three erection stages as illustrated in Figure 10. For stage A1, the median barrier was removed; A2, median barrier and fairings removed; A3, median barrier, fairings, and railings removed. Horizontal pressures were computed from the coefficients for a moderate wind angle of $+2^\circ$ and were found to be somewhat less than recommended AASHTO values for configuration C-2C-A and about equal to the AASHTO values for stage A2.

Conclusions

This paper summarizes the results of comprehensive wind tunnel studies of two major bridge structures. The two bridges studied are examples of the cable-stayed, box-girder type which, until recently, has not often been constructed in the United States. In general, all the cross sections tested in a horizontal wind have critical velocities for flutter in excess of the appropriate design wind speeds. At other wind inclinations, the critical velocities remain high enough to exceed expected winds. Varying degrees of vertical motion are caused by vortex shedding at speeds between 24 and 48 km/h (15 and 30 mph). For the Luling, Louisiana, Bridge, vertical vortex shedding response amplitudes and accelerations are minimal and considered neither damaging to the structure nor discomforting to the user. In the case of the Huntington, West Virginia, Bridge, vortex-induced oscillations also are not a threat to bridge safety; however, due to the larger accelerations, pedestrians or passengers in stationary vehicles may feel some vertical motion. Drag forces measured in the wind tunnel appear reasonable relative to recommended design values. Further

details regarding this research may be found in the two recent study reports: "Aerodynamic Investigations of the Luling, Louisiana, Cable-Stayed Bridge," FHWA-RD-77-161 and "Aerodynamic Stability of Proposed Ohio River Cable-Stayed Bridge," FHWA-RD-77-157.

Acknowledgments

These projects were carried out at the request of the Louisiana Department of Transportation and Development and West Virginia Department of Highways. The authors gratefully acknowledge the technical support and guidance provided by Mr. Richard H. Gade, Project Manager for FCP Project 5A. Despite Mr. Gade's failing health in recent years, he never ceased to serve as a guiding force on these and other projects in the Wind Engineering field. Regretfully, Mr. Gade died on September 25, 1977, and he will be deeply missed by all those who knew him.

References

1. F. B. Farquharson et al. Aerodynamic Stability of Suspension Bridges with Special Reference to the Tacoma Narrows Bridge. University of Washington Engineering Experiment Station, Bulletin No. 116, Parts I-V, June 1949 to June 1954.
2. R. H. Gade and R. H. Scanlan. Experimental Measurement and Interpretation of Aerodynamic Stability Coefficients for the Decks of Two Cable-Stayed Bridges. Proceedings of ASCE and EMD Symposium on Dynamic Response of Structures, UCLA, March 1976, pp. 478-486.
3. R. H. Scanlan and J. J. Tomko. Airfoil and Bridge Deck Flutter Derivatives. Journal of Engineering Mechanics, Vol. 97, ASCE, December 1971, pp. 1717-1737.
4. R. H. Scanlan. Recent Methods in the Application of Test Results to the Wind Design of Long, Suspended-Span Bridges. Federal Highway Administration, Report No. FHWA-RD-75-115, October 1975.
5. R. H. Gade, H. R. Bosch, and W. Podolny, Jr. Recent Aerodynamic Studies of Long-Span Bridges. Journal of the Structural Division, Vol. 102, ASCE, July 1976, pp. 1299-1315.

Table 1. Cross-sectional data.

Section model designation (1)	Prototype section depth, in feet (2)	Roadway surface (3)	Railing type (4)	Vertical natural frequency, in cycles per second (5)	Torsional natural frequency, in cycles per second (6)
C-2-C-1	14	Concrete	Basic	2.62	5.29
C-2-C-2	14	Concrete	Alternate	2.56	5.20
C-2C-C	14	Concrete	Alternate	2.56	5.35
C-2C-A	14	Asphalt	Alternate	2.80	5.25
C-2A-C-1	12	Concrete	Basic	2.53	5.24
C-6-C-B	14	Concrete	Basic	2.49	5.33
C-6-C-A	14	Concrete	Alternate	2.48	5.24
3-2.4-.01	9.6	Asphalt	Basic	2.51	6.80

1 ft = 0.3048m

Figure 1. Bridge elevation and cross sections - Luling, La. Bridge.

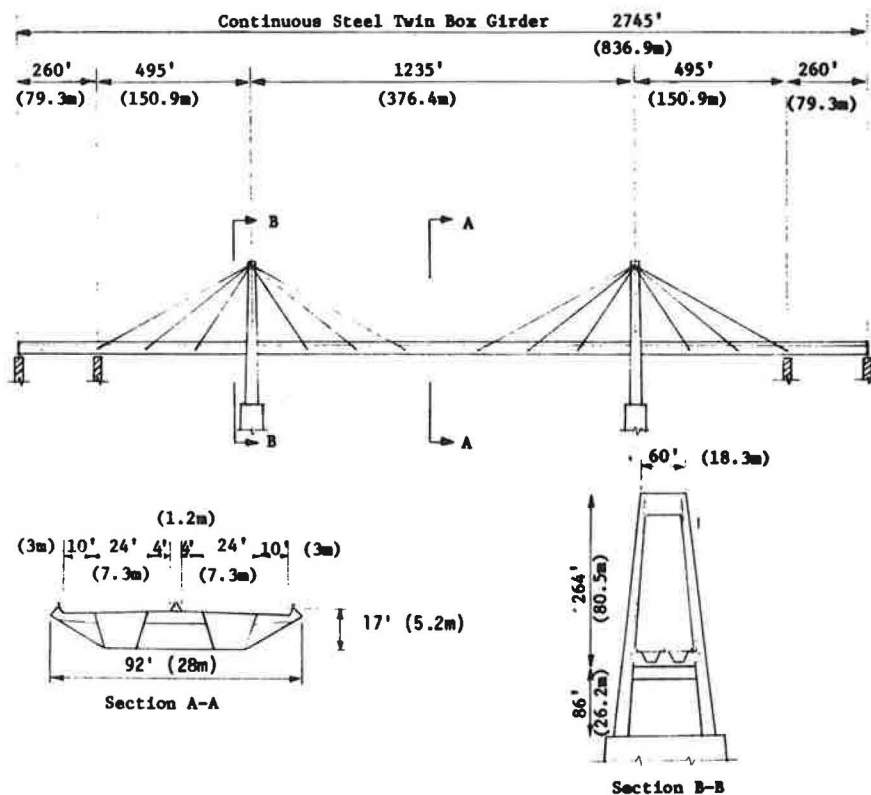


Figure 2. General elevation of prototype - Huntington, W. Va. Bridge.

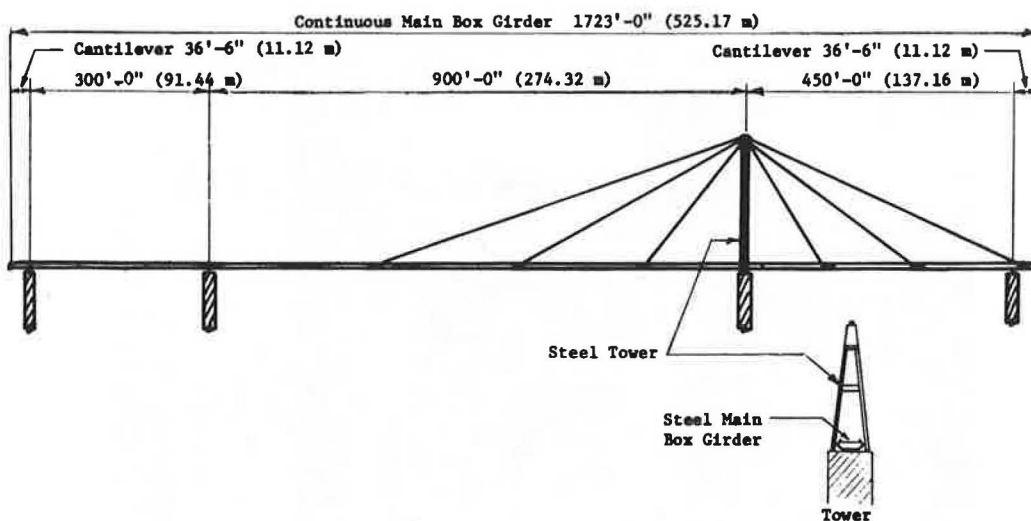
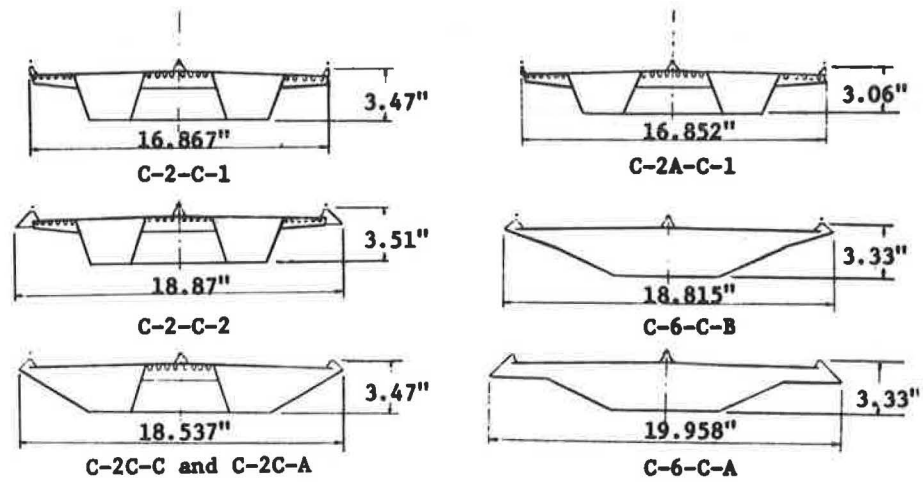
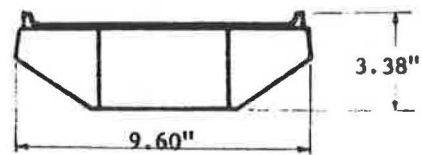


Figure 3. Model configurations and dimensions (1 inch = 25.4 mm).



Luling, La. 1:60 Scale Section Models



3-2.4-.01

Huntington, W.VA. 1:45 Scale Section Model

Figure 4. Model in wind tunnel.

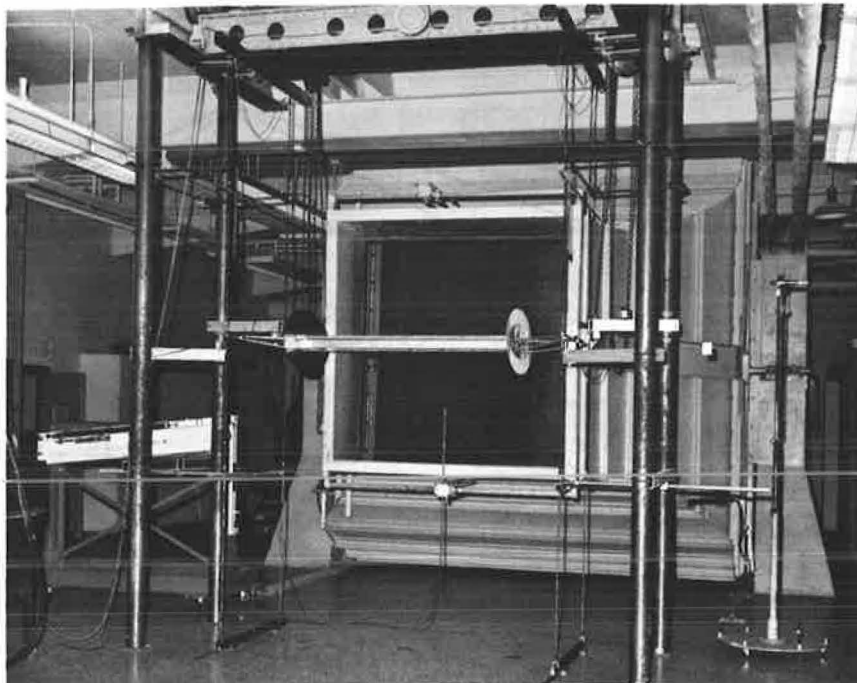


Figure 5. Flutter derivative for vertical - angle of attack = 0°.

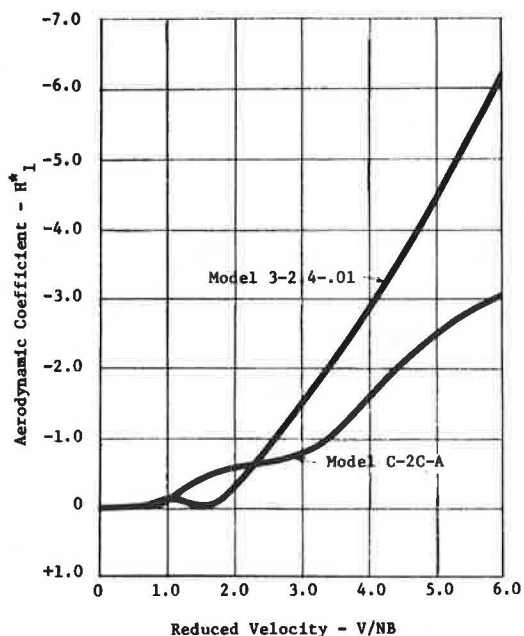


Figure 6. Critical flutter velocity - no damping.

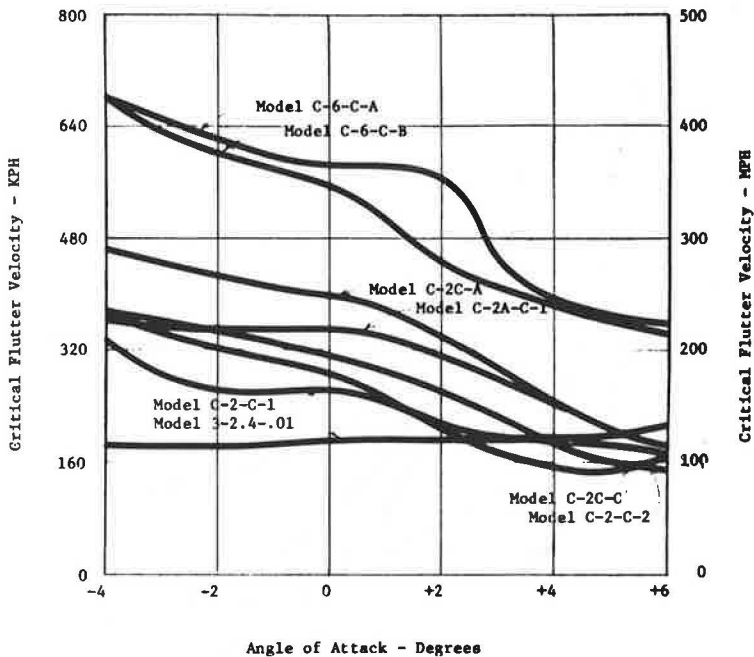


Figure 7. Critical flutter velocity - 1/8 critical damping.

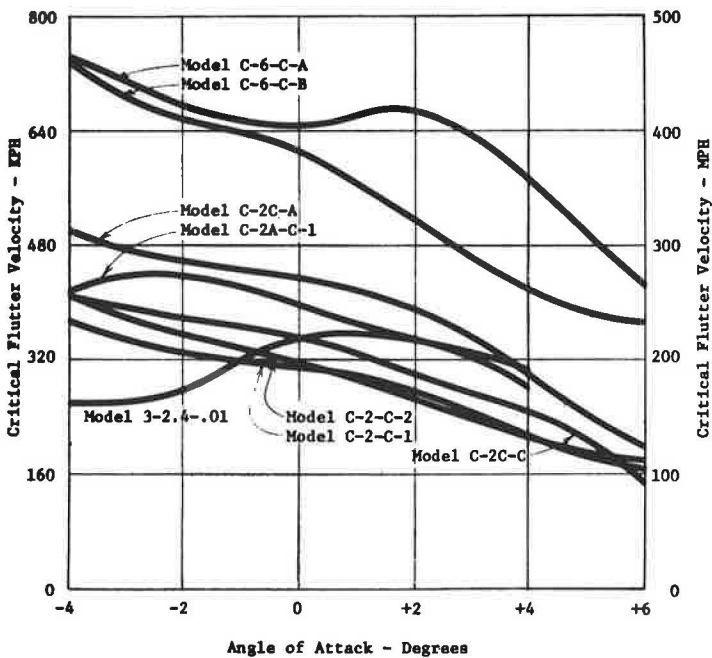


Figure 8. Flutter derivative for torsion - angle of attack = 0°.

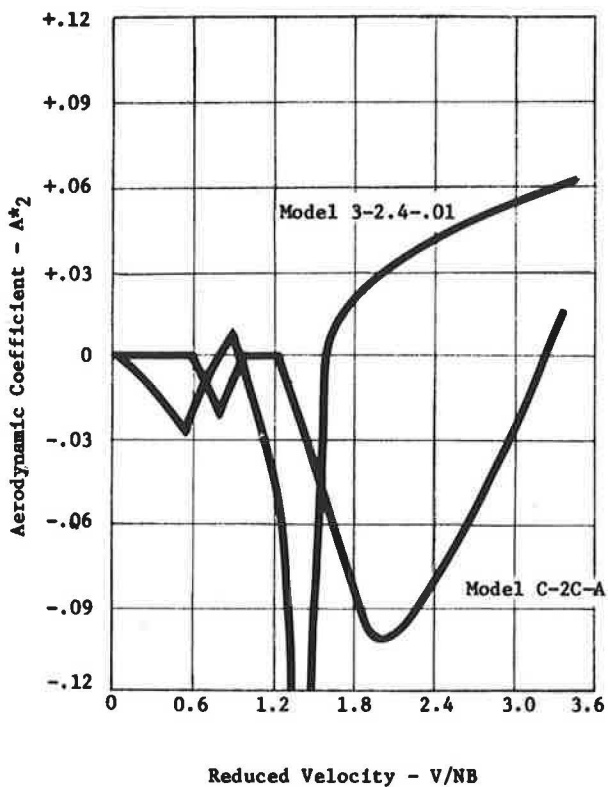


Figure 9. Estimate of prototype accelerations resulting from vertical vortex excitation - angle of attack = 0°.

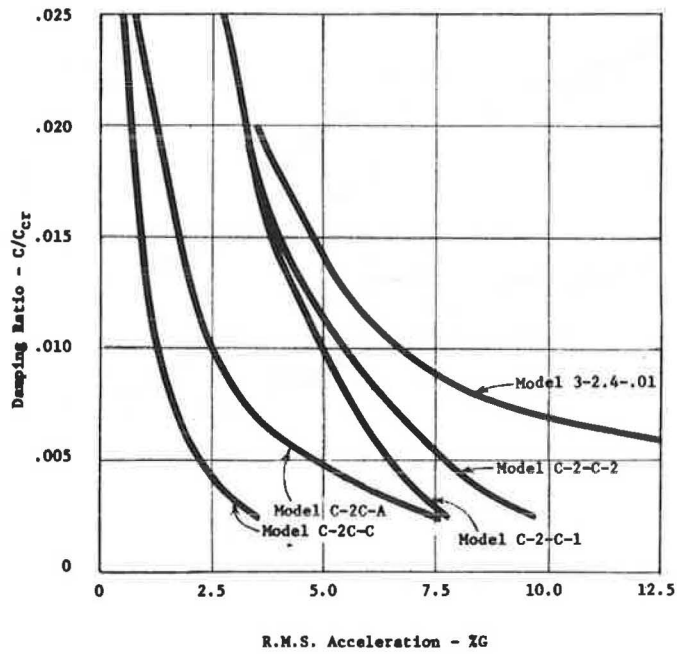


Figure 10. Drag coefficients.

